



ELSEVIER

Available online at [www.sciencedirect.com](http://www.sciencedirect.com)

SCIENCE @ DIRECT®

Journal of Magnetism and Magnetic Materials 300 (2006) 427–435



[www.elsevier.com/locate/jmmm](http://www.elsevier.com/locate/jmmm)

# The $Z_2$ phase transition in the fully frustrated XY model as a percolation problem

A.B. Lima\*, B.V. Costa

*Departamento de Física ICEX, Universidade Federal de Minas Gerais, Laboratório de Simulação, Caixa Postal 702, 30123-970 Belo Horizonte-MG, Brazil*

Received 7 March 2005; received in revised form 20 May 2005

Available online 21 June 2005

---

## Abstract

The fully frustrated planar rotator and fully frustrated XY models in two dimensions have two phase transitions: one of the Berezinskii–Kosterlitz–Thouless type and other in the Ising universality class. We use Monte Carlo simulation to study both models. We fix our attention in the Ising-like transition, which we show can be understood as a percolation transition. We obtain the critical temperature as well as the critical exponents of the mean cluster size,  $\gamma$ , and Fisher's exponent  $\tau$ . The critical temperature agree very well with other calculations. We found that the critical exponents are smaller than in the pure two-dimensional percolation case. We interpret this as due to the long-range interaction between vortex and antivortex.

© 2005 Elsevier B.V. All rights reserved.

PACS: 64.60.Cn; 74.80.-g; 75.10.Hk

Keywords: Percolation; XY model

---

## 1. Introduction

Phase transitions are classified by symmetries of order parameters and spatial dimensionality to universality classes, each of which having a particular set of critical exponents [1]. Of particular interest are continuous magnetic models in

two dimensions realized as the XY and planar rotator (PR) models [2–10]. Those are special models in magnetism. They undergo an unusual phase transition to a state with bound, topological excitations: vortex–antivortex pairs. A vortex (antivortex) is a topological excitation in which spins on a closed path around the excitation core process by  $f\pi$  ( $-f\pi$ ) with  $f = 1, 2$ , in the same direction. The models do not exhibit any true long-range order. This lack of long-range order follows from the Mermin–Wagner theorem [11], which

---

\*Corresponding author. Tel.: +55 313 499 5648; fax: +55 313 499 5600.

E-mail address: [alima@fisica.ufmg.br](mailto:alima@fisica.ufmg.br) (A.B. Lima).

asserts that a broken continuous symmetry prevents long-range order for continuous spin models in two dimensions. The models, however, do undergo a phase transition at a finite temperature  $T_{\text{BKT}}$ , from a high-temperature phase where the correlation function exhibits an exponential decay to a low-temperature phase with quasi-long-range order where the correlation function has a power-law decay. This phase transition is believed to be driven by a vortex–antivortex unbinding mechanism. The mechanism of the phase transition was first illustrated by Berezinskii and Kosterlitz and Thouless [12,13] (BKT): at low-temperature spin waves are the only significant excitations, and vortices are bound in pairs, not affecting the spin wave description quantitatively. However, as temperature grows the binding of vortices decreases and free vortices can be found in the system. Isolated vortices are global excitations, so that, they affect the entire system increasing its entropy. At  $T_{\text{BKT}}$  it undergoes a BKT phase transition. Because the free energy of the system is an analytical function this phase transition is said to be in an infinite order phase transition class. Of particular interest are the fully frustrated versions of the PR (FFPR) and XY (FFXY) models in two dimensions [2–4,6,7,10,14–16]. On the contrary of the unfrustrated models which cannot present any true long-range order at any finite temperature, frustrated models are expected to display a richer critical behavior due to two different symmetries present. Beside the continuous spin symmetry which leads to a BKT transition it poses a  $Z_2$  symmetry corresponding to a vortex–antivortex condensate in the ground state. The appearing of this symmetry leads to the possibility of long-range order. In this report we investigate the FFPR and the FFXY models in two dimensions by using numerical techniques. The FFPR model is defined as

$$H_{\text{PR}} = \sum_{\langle i,j \rangle} J_{ij} \cos(\theta_i - \theta_j), \quad (1)$$

where  $i$  and  $j$  enumerate lattice sites,  $\theta_i$  is the angle at the lattice point  $i$  and  $J_{ij}$  is an exchange coupling which is ferromagnetic in all lines in the  $x$  direction and is alternately ferromagnetic and antiferromagnetic in the  $y$  direction. For the

FFXY we define

$$H_{\text{XY}} = \sum_{\langle i,j \rangle} J_{ij} \vec{S}_i \vec{S}_j + \sum_{\langle i,j \rangle} A_{ij} S_i^z S_j^z, \quad (2)$$

where  $\vec{S}_i = S_i^x \hat{x} + S_i^y \hat{y} + S_i^z \hat{z}$  is a Heisenberg spin vector at site  $i$  and  $A_{ij} > 0$ , with  $J_{ij}$  defined as in the FFPR model. Due to the easy plane anisotropy  $A$ , the Heisenberg symmetry is broken leading the system to have the same symmetry as the FFPR model. The coupling distribution imposes to the ground state a checkerboard pattern of plaquettes with positive (vortex) or negative (antivortex) chirality,  $f$ , given by (see Fig. 1)

$$f = \frac{1}{\pi} \sum_{\text{plaquette}} (\phi_i - \phi_j) = \pm 1. \quad (3)$$

Here,  $\phi$  is the angle between the XY spin vector component and some fixed direction in the plane. Both models, FFPR and FFXY, are in the same universality class. The ground state of the models have a continuous degeneracy due to the spin symmetry and a  $Z_2$  degeneracy due to the  $f$  degrees of freedom. These symmetries may led the system to have two phase transitions, one at  $T_{Z_2}^{\text{PR,XY}}$  and other at  $T_{\text{BKT}}^{\text{PR,XY}}$ . In the first Monte Carlo (MC) simulation of the FFPR model Teitel and Jayaprakash [4] found a steep drop in the helicity modulus, signaling a BKT transition, accompanied by an increase in the specific heat with lattice size, consistent with an  $Z_2$  transition. However, the authors being not able to determine the precise critical behavior of the model, suggested the following possible scenarios:

1. The loss of  $Z_2$  and XY order take place at the same temperature  $T_{\text{BKT}} = T_{Z_2}$ .
2. The  $Z_2$  transition occurs at a higher temperature than the BKT transition.

Since then, several studies have been made on the model to decide between these two possibilities (see Ref. [10] and references therein). Some of the earliest MC investigations suggested that the  $Z_2$  critical exponents could be different from the pure Ising ones, opening the possibility to the model to

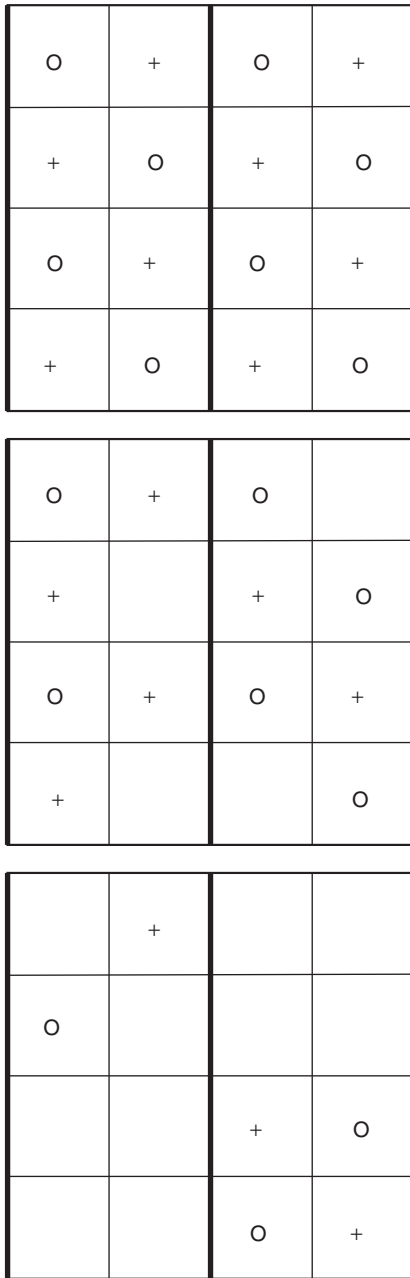


Fig. 1. Sequence of snapshots representing the vortex–antivortex equilibrium configurations for three different temperatures,  $T < T_{\text{BKT}}$ ,  $T \approx T_{\text{BKT}}$  and  $T > T_{\text{BKT}}$  for the fully frustrated model. The thin and thick lines represent ferromagnetic and antiferromagnetic coupling, respectively.

be in a new universality class. Peter Olson [10], in a very extensive MC calculation, reported the critical temperatures of the FFPR model as  $T_{\text{BKT}}^{\text{PR}} \approx 0.446\text{J}$  and  $T_{Z_2}^{\text{PR}} \approx 0.452\text{J}$ . He found genuine Ising exponents to the  $Z_2$  transition and argued that the non-Ising exponents found by others is due to a failure of the used finite size scaling. In recent papers Korshunov [7] argued that the BKT transition should occur at lower temperature than the  $Z_2$  transition. More recently, Lima and Costa [17] calculated the critical temperatures for the FFPR and FFX models finding  $T_{\text{BKT}}^{\text{PR}} = 0.4410(5)\text{J}$ ,  $T_{Z_2}^{\text{PR}} = 0.4511(10)\text{J}$  and  $T_{\text{BKT}}^{\text{XY}} = 0.3655(5)\text{J}$ ,  $T_{Z_2}^{\text{XY}} = 0.3690(3)\text{J}$ , respectively, confirming the results of Olson and Korshunov. The FF models can be seen as diluted models since at  $T = 0$  each plaquette supports a vortex or antivortex. As temperature grows, the vortex (antivortex) acquire enough energy to jump to another plaquette occupied by an antivortex (vortex) such that they annihilate each other. This has the effect to diminish the vortex density. Considering that vortices can move changing their positions with vortex free plaquettes in order to minimize the free energy of the system, we have an annealed like site diluted Ising model to deal with [18]. The difference from a conventional Ising model is due to the possibility of fluctuations in the vortex density for fixed temperature: a pair vortex–antivortex can be created or annihilated. Rigorous inequalities were proved by Coniglio et al. [19], which relate percolation probability to critical points in quenched Ising models. In two dimensions the critical point was shown to be a percolation point. As the FF models have a  $Z_2$  transition, we expect that critical thermodynamic quantities are related to the percolation ones.

In this paper we present MC results for the  $Z_2$  transition in the FFPR and FFX models. Our analysis is based on the properties of the vortex percolation probability at the critical  $Z_2$  temperature. This work is organized as follows. In Section 2 we discuss in detail the critical properties of both models: FFPR and FFX. In Section 3 we present some details of the numerical simulation. In Sections 4 and 5 we show our results and conclusions, respectively.

## 2. Background

Due to the coupling distribution between sites in the FFPR and FFXY models, their ground state present a checkerboard distribution of vortices, being the center of the vortices located at the center of each plaquette. The associated parameter  $f$ , which characterize the vorticity, has a  $Z_2$  symmetry playing the role of an Ising variable. We can associate the  $f$  variable to each site of the dual lattice in such way that the ground state is the same as in an Ising antiferromagnetic model. At zero temperature ( $T = 0$ ), the vortex density in the system is  $\rho^{\text{XY,PR}} = 1$ . Once the temperature grows, pairs vortex–antivortex start to annihilate each other, so that, its density diminish as shown in Figs. 1 and 2.

We observe that close to the transitions there is a sharp drop in the vortex density. In Fig. 3 we show the derivative,  $d\rho/dT$ , obtained by MC simulations for several lattice sizes as discussed in Ref. [17]. At some value  $T_L$  each curve presents a maximum. An extrapolation for  $L \rightarrow \infty$  gives  $T_{L \rightarrow \infty}^{\text{PR}} = 0.453(5)\text{J}$  and  $T_{L \rightarrow \infty}^{\text{XY}} = 0.369(4)\text{J}$ , as seen in Fig. 4, which matches  $T_{Z_2}^{\text{PR}}$  and  $T_{Z_2}^{\text{XY}}$ , respectively, inside the error bars, as discussed in Ref. [17]. This behavior is not observed in the non frustrated models. At the  $Z_2$  transition we expect  $\rho^{\text{XY,PR}}(T_{Z_2}) = \rho_c^{\text{XY,PR}}$ , where  $\rho_c^{\text{XY,PR}}$  is to be identified with the percolation threshold. We will turn back to this point later.

We can expect that at the critical concentration  $\rho_c^{\text{XY,PR}}$ , the percolation threshold is attained, so that, below this concentration the system cannot support any transition at all. In principle, if the  $Z_2$  transitions were genuine Ising transitions, we should expect the critical concentration to be  $\rho^{\text{XY,PR}} \approx 0.593$  for both models with the well-known classical percolation exponents:  $\alpha = -\frac{2}{3}$ ,  $\beta = \frac{5}{36}$ ,  $\gamma = \frac{43}{18}$ ,  $\tau = \frac{187}{91}$  and so on. However, since the vortex–(anti)vortex interaction is logarithmic we cannot expect any exact match. Beside that, due to the logarithmic range of interaction, we have to face the problem of defining the concept of neighborhood which is central to the calculation of any quantity in percolation theory. This question was discussed by Costa et al. in Ref. [20], in the context of the nonfrustrated XY model. In short,

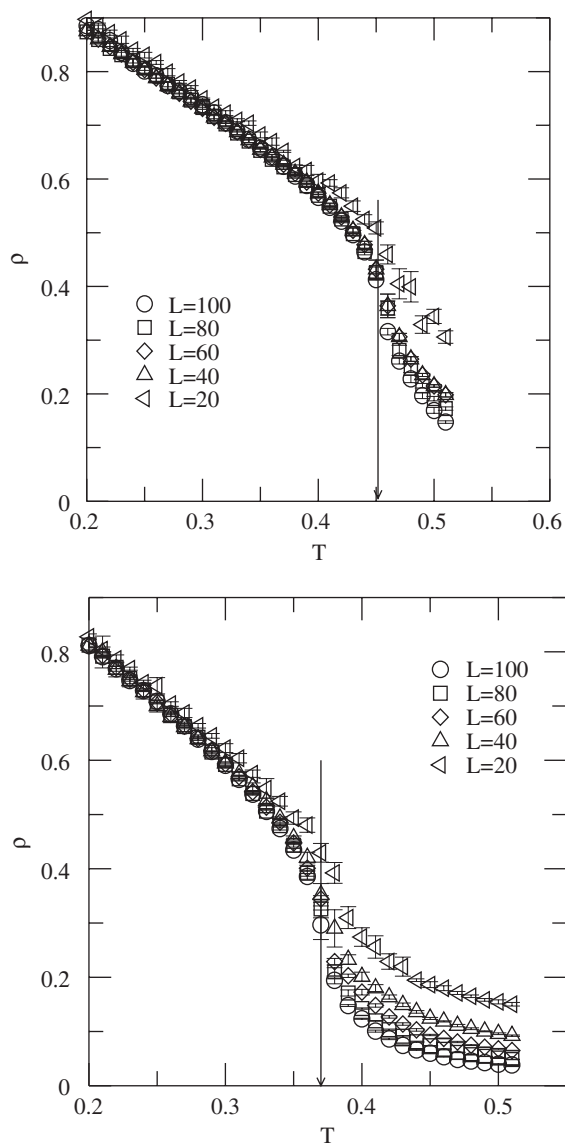


Fig. 2. Figures are for the vortex density,  $\rho^{\text{XY,PR}}$ , as a function of temperature for several lattice sizes as indicated in the legends. We observe that  $\rho^{\text{XY,PR}}$  suddenly drops at some temperature  $T_L^{\text{XY,PR}}$ . The arrows represent the critical temperatures  $T_{Z_2}^{\text{PR}} = 0.4511$  and  $T_{Z_2}^{\text{XY}} = 0.3690$ . The top and bottom figures are for the PR and XY models, respectively.

they have calculated the position of all vortices and antivortices in the system for several temperatures. By measuring the distance between every vortex–antivortex pair they considered as nearest

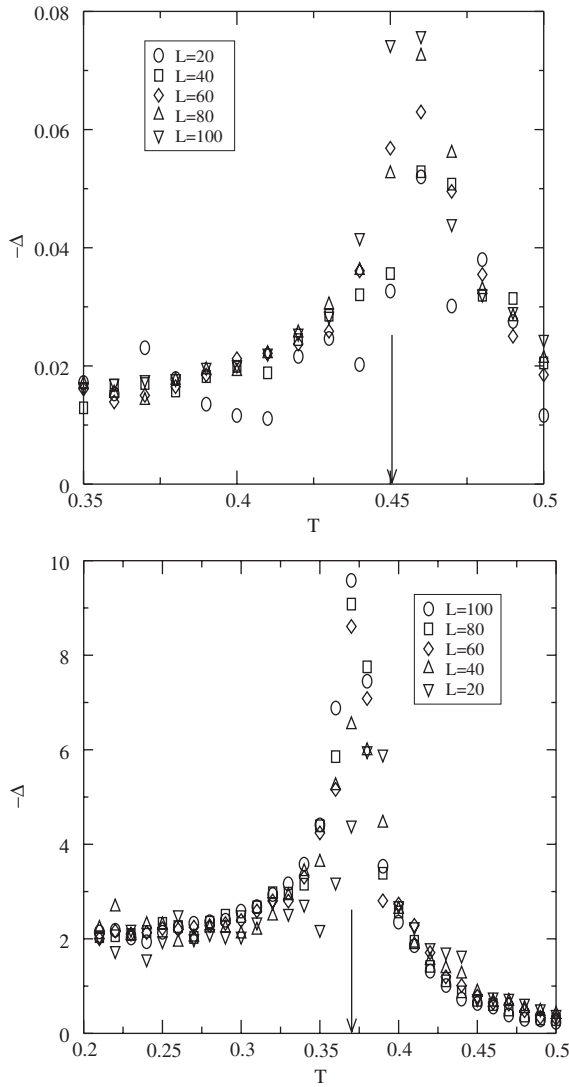


Fig. 3. The figures represent the derivatives of the vortex density as a function of temperature. The sequence of the figures are the same as in Fig. 2.

neighbor pairs those at the smallest distance,  $d_{v-av}$ . By analyzing  $d_{v-av}$  as a function of temperature they found that the pair size has no discontinuous behavior upon passing through the transition, but it grows continuously with temperature. In the low-temperature phase (low vortex density in the non frustrated case), the maximum distance between vortex–antivortex in the pair was found to be about three lattice spacings. We remind

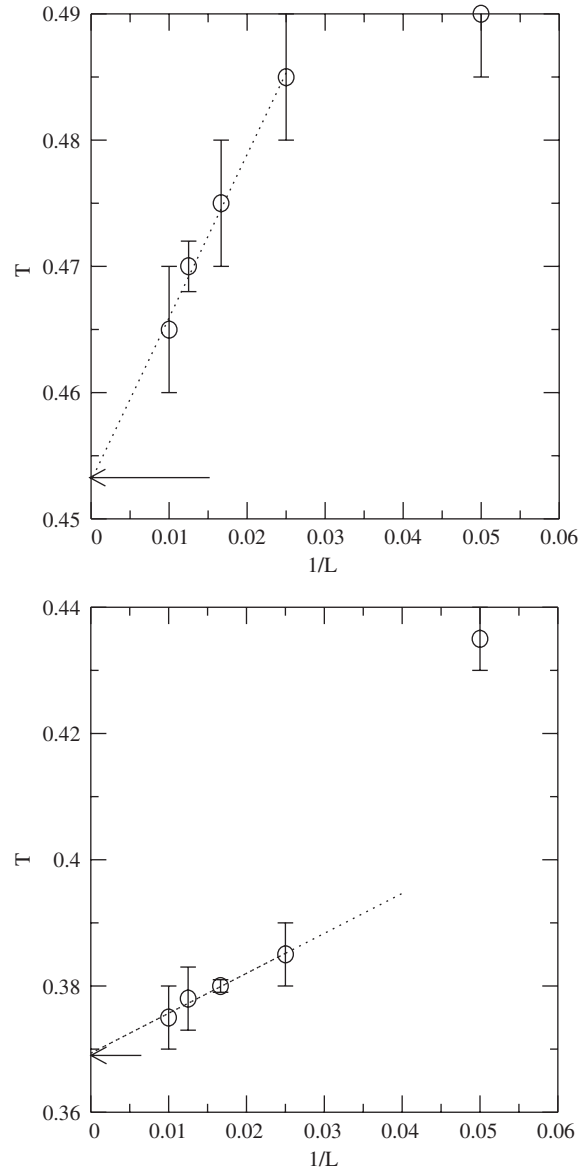


Fig. 4. The figures represent the maxima of the derivatives of the vortex density as a function of  $L^{-1}$ . The dotted lines are extrapolation for  $L \rightarrow \infty$ , which gives  $T_L^{PR} = 0.453(5)$  and  $T_L^{XY} = 0.369(4)$ . Those values are shown as arrows.

ourselves that in the low-temperature phase vortices are supposed to be bounded, following the Kosterlitz–Thouless transition picture. With this in mind, it is reasonable to suppose that two spins are neighbors if they are up to three lattice

spaces apart. If we can obtain  $\rho_c^{\text{XY,PR}}$  we immediately obtain  $T_{Z_2}^{\text{XY,PR}}$  through Fig. 2, since it gives the density as a function of temperature.

Two important quantities in percolation theory are the mean cluster size,  $S_{\text{av}}$ , and the percolation probability  $P$  [18]. The mean cluster size is defined as

$$S_{\text{av}} = \frac{\sum_{s=1}^{\infty} s^2 n(s)}{\sum_{s=1}^{\infty} s n(s)}, \quad (4)$$

where  $s$  is the number of clusters of size  $n(s)$ . Close to the percolation threshold it behaves as

$$S_{\text{av}} \sim (\rho_c - \rho)^{-\gamma} \quad (\rho \rightarrow \rho_c). \quad (5)$$

By measuring  $S_{\text{av}}$  we can estimate the critical concentration  $\rho_c$  and the critical exponent  $\gamma$ .

Another important quantity is the percolation probability  $P$  which measures the probability of a cluster to percolate. It must be a step function: for  $\rho < \rho_c$ ,  $P = 0$  and  $P = 1$  for  $\rho > \rho_c$ , so that a plot of  $P$  as a function of  $\rho$ , immediately gives an estimate of  $\rho_c$ . The asymptotic behavior of the cluster numbers,  $n_s(\rho_c)$ , defines Fisher's exponent  $\tau$ . For large  $s$  it behaves as

$$n_s(\rho_c) \propto s^{-\tau}. \quad (6)$$

In the next section we will use MC simulation to calculate the quantities we discussed above.

### 3. Numerical details

We have studied the two-dimensional classical fully frustrated XY and PR models with Hamiltonian given in Eq. on  $L \times L$  lattices with periodic boundary conditions for  $20 \leq L \leq 100$  for several temperatures below and above the  $T_{Z_2}^{\text{XY,PR}}$  transition.

Equilibrium configurations were created at each temperature using a MC vectorized Metropolis method. Although, cluster algorithms are much faster than Metropolis for nonfrustrated versions of the model [21], it does not work quite well in frustrated situations, such that, we found more convenient to use the Metropolis algorithm here. We discarded the first  $100 \times L \times L$  sweeps for equilibration, since that, averages of basic quantities as energy, specific heat and susceptibilities

variate less than 0.2%, using the specified criterium.

Between  $10^3$  and  $10^4$  equilibrium configurations were generated for each lattice size and temperature. We found this many configurations to be necessary in order to sufficiently reduce statistical errors in the resulting counting of percolating clusters close to  $T_{Z_2}^{\text{XY,PR}}$ . The error bars in our figures represent the statistical errors for averages over the equilibrium configurations, drawn from the canonical ensemble.

To get both, the number and the cluster size we have used the Hoshen and Kopelman algorithm [18].

### 4. Results

We now present our results for the critical temperatures  $T_{Z_2}^{\text{PR}}$  and  $T_{Z_2}^{\text{XY}}$ , the mean cluster size  $S_{\text{av}}$ , and the critical exponent  $\gamma$ , the percolation probability  $P$  and Fisher's exponent  $\tau$ .

Fig. 3 shows the negative of the derivative of the vortex density as a function of temperature for several lattice sizes. Each curve exhibits a sharp maximum at some temperature  $T_L^{\text{PR,XY}}$ . By plotting  $T_L^{\text{PR,XY}}$  as a function of the lattice size  $L$ , we can adjust a straight line to our data (see Fig. 4). An extrapolation to  $L \rightarrow \infty$  gives  $T_{\infty}^{\text{PR}} = 0.453(5)$  and  $T_{\infty}^{\text{XY}} = 0.369(4)$ , which are to be compared to  $T_{Z_2}^{\text{PR}} = 0.4511(10)$  and  $T_{Z_2}^{\text{XY}} = 0.3690(3)$ , obtained by Lima and Costa [17] using a thermodynamic approach. The same numbers are found by using the percolation probability as a function of temperature as shown in Fig. 5. An estimate of the critical temperature gives  $T_p^{\text{PR}} = 0.451(5)$  and  $T_p^{\text{XY}} = 0.369(5)$ .

Fig. 6 shows a log–log plot of the average cluster size distribution as a function of density for  $\rho < \rho_c$  and  $\rho > \rho_c$ . Following Ref. [18] we obtain for the critical exponent  $\gamma^{\text{PR}} = 2.07(5)$  and  $\gamma^{\text{XY}} = 2.08(5)$ . Those values agree between themselves but are below the quenched two-dimensional site diluted percolation model  $\gamma = \frac{43}{18} \approx 2.39$ .

Fisher's exponent,  $\tau$ , can be obtained by plotting the cluster number  $n_s$  as a function of the cluster size  $s$ . From Fig. 7 we obtain  $\tau^{\text{PR}} = 1.89(5)$  and  $\tau^{\text{XY}} = 1.77(5)$ . Again, the values agree between

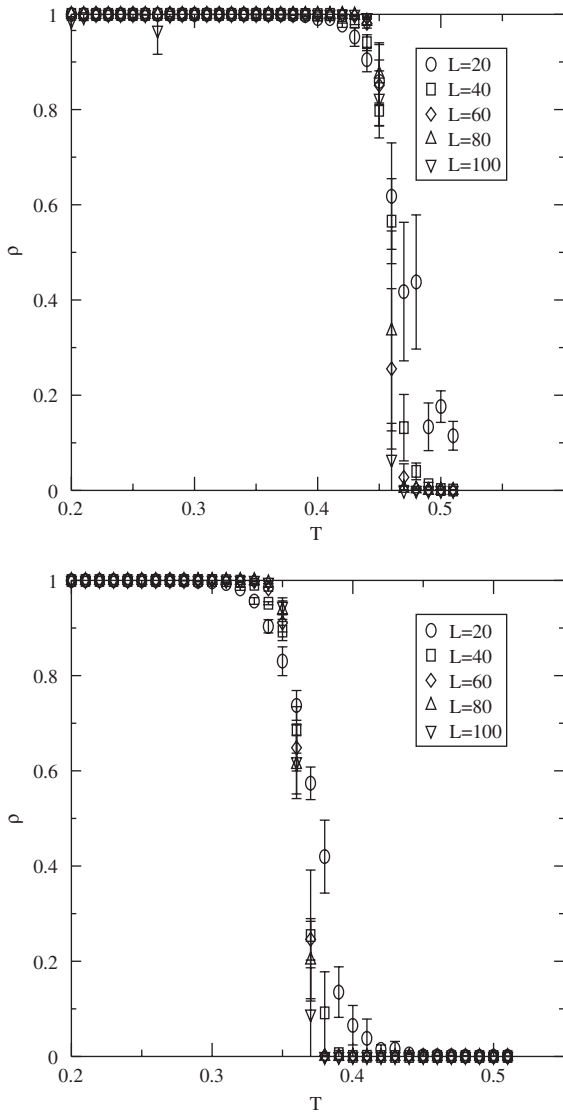


Fig. 5. Percolation probability as a function of temperature.

themselves but are below  $\tau = \frac{187}{91} \approx 2.05$ , which is the exact value for the two-dimensional case.

### 5. Conclusions

We observed that the inflection point in the vortex density gives a very good estimate of the  $T_{Z_2}^{XY,PR}$ . The question is to know if this coincidence

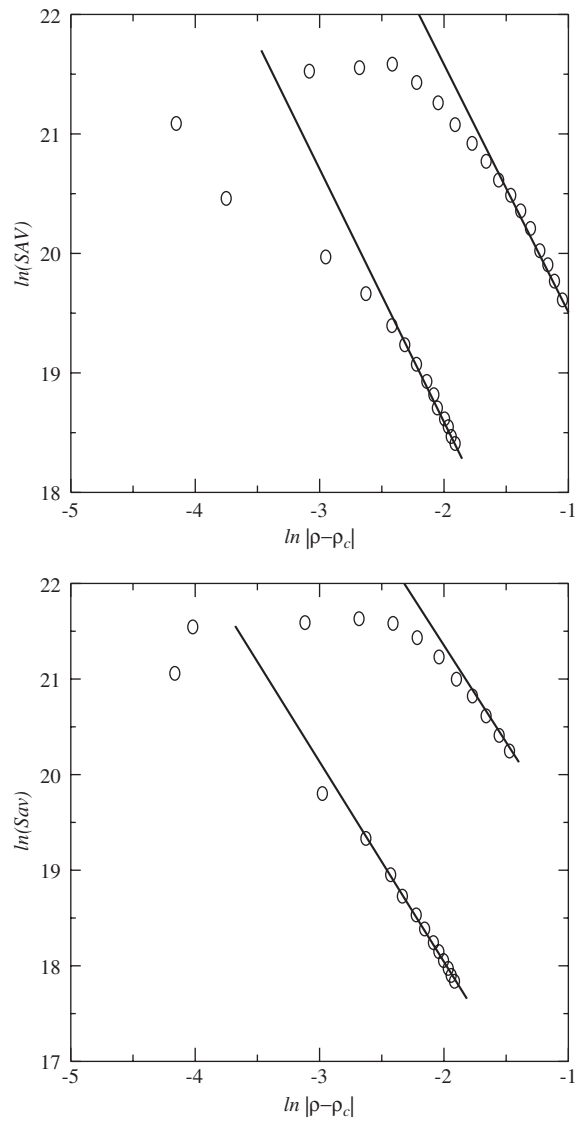


Fig. 6. Log–log plot of the average cluster size distribution as a function of density. The straight lines are linear adjusts. The upper curve is for  $\rho < \rho_c$  and the other for  $\rho > \rho_c$ . The top and bottom graphics is for PR and XY models, respectively.

is incidental or not. Although we cannot rigorously prove, a reasonable explanation for that is as follows. At  $T = 0$  there are  $L \times L/2$  vortex pairs in the lattice. Once the temperature grows, they are activated, so that, some pairs can acquire enough energy to be annihilated. The vortex density diminish as temperature grows. When the BKT



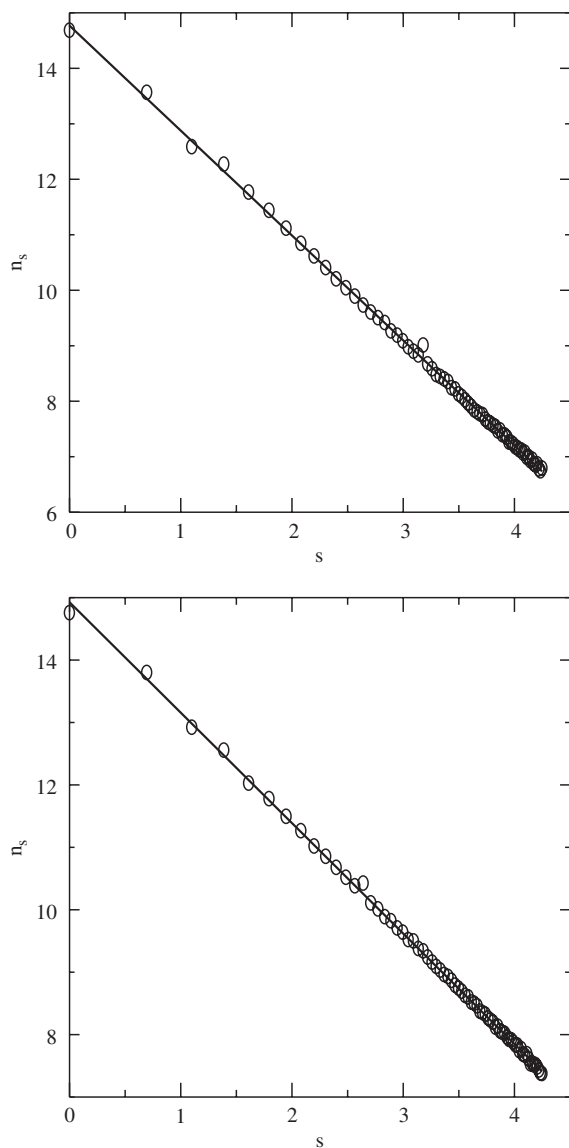


Fig. 7. Cluster number  $n_s$  as a function of the cluster size  $s$ . The solid straight lines are the result of the best adjust to the data.

temperature is reached, pairs are weakly bounded. The spin waves shield the vortex interaction, however, they cannot be considered as free, since its interaction is still logarithmic. Just after the BKT transition temperature the thermal energy is high enough, so that, it equals the pinning energy due to the lattice discreteness, inducing a cascade of annihilations and giving origin to the sudden

drop in the vortex density. As a consequence of the severe diminishing of the vortex number, the vortex density goes below the percolation threshold which on the other hand leads to the  $Z_2$  transition.

Our calculations of the mean cluster size and the percolation threshold allows us to calculate the critical temperatures  $T_{Z_2}^{XY,PR}$  and two critical exponents:  $\gamma$  and  $\tau$ . The values for the critical temperatures we have obtained are in excellent agreement with other calculations. For the critical exponents, the values are different from the pure two-dimensional cases. There are several reasons for that. The models we have found in the literature refer to quenched situations, while ours is an annealed model. In general, interactions are short ranged in those models, justifying a first neighbor approach. Here, due to the logarithmic potential we have to consider interactions up to the third neighbor.

The Fisher's exponent,  $\tau$ , is obtained by the Cluster number  $n_s$ .

The other critical exponents can be obtained from the universal relations,  $2 - \alpha = (\tau - 1)/\sigma = 2\beta + \gamma$  and  $\tau = (2 + \beta)/(\beta + \gamma)$ . Unfortunately, we have not been able to calculate independently at least one more exponent which could allow us to confirm (or not) the universal relations between the critical exponents.

### Acknowledgements

This work was partially supported by CNPq and FAPEMIG (Brazilian agencies). Numerical work was done in the LINUX parallel cluster at the *Laboratório de Simulação* Departamento de Física—UFMG.

### References

- [1] L.P. Kadanoff, W. Götze, D. Hamblen, R. Hecht, E.A.S. Lewis, V.V. Palciauskas, M. Rayl, J. Swift, D. Aspnes, J. Kane, *Rev. Mod. Phys.* 39 (1967) 395.
- [2] J. Villan, *J.Phys. C* 10 (1977) 4793.
- [3] T. Ohta, D. Jasnow, *Phys. Rev. B* 20 (1979) 139.
- [4] S. Teitel, C. Jayaprakash, *Phys. Rev. Lett.* 51 (1983) 1999.
- [5] P. Minnhagen, *Rev. Mod. Phys.* 59 (1987) 1001.



- [6] J.-R. Lee, S.J. Lee, B. Kim, I. Chang, *Phys. Rev. Lett.* 79 (1997) 2172.
- [7] S.E. Korshunov, *Phys. Rev. B* 63 (2001) 134503-1-5; S.E. Korshunov, *Phys. Rev. Lett.* 88 (2002) 167007-1-4.
- [8] B.V. Costa, S.S.T. Pires, *Phys. Rev. B* 64 (2001) 92407-1-4; B.V. Costa, A.S.T. Pires, *J. Magn. Magn. Mater.* 262 (2003) 316.
- [9] S.A. Leonel, P.Z. Coura, A.R. Pereira, L.A.S. Mól, B.V. Costa, *Phys. Rev. B* 67 (2003) 104426-1-5.
- [10] P. Olsson, *Phys. Rev. Lett.* 73 (1994) 3339; P. Olsson, *Phys. Rev. B* 52 (1995) 4526; P. Olsson, *Phys. Rev. B* 77 (1996) 4850; P. Olsson, *Phys. Rev. B* 55 (1997) 3585.
- [11] N.D. Mermin, H. Wagner, *Phys. Rev. Lett.* 17 (1966) 1133.
- [12] V.L. Berezinskii, *Zh. Eksp. Teor. Fiz.* 6 (1971) 1144.
- [13] J.M. Kosterlitz, D.J. Thouless, *J. Phys. C* 6 (1973) 1181; J.M. Kosterlitz, *J. Phys. C* 7 (1974) 10446.
- [14] G.S. Grest, *Phys. Rev. B* 39 (1989) 9267.
- [15] E. Granato, J.M. Kosterlitz, J. Lee, M.P. Nightingale, *Phys. Rev. Lett.* 68 (1992) 1224.
- [16] G. Ramirez-Santiago, J.V. José, *Phys. Rev. B* 49 (1994) 9567.
- [17] A.B. Lima, B.V. Costa, *J. Magn. Magn. Mater.* 263 (2003) 324; A.B. Lima, B.V. Costa, *Braz. J. Phys.* 34 (2004) 403.
- [18] D. Stauffer, A. Aharony, *Introduction to Percolation Theory*, Taylor & Francis Inc., London, 1992.
- [19] A. Coniglio, C.R. Nappi, F. Peruggi, L. Russo, *J. Phys. A* 10 (1977) 205.
- [20] J.E.R. Costa, D.P. Landau, B.V. Costa, *Phys. Rev. B* 57 (1998) 11510.
- [21] H.G. Evertz, D.P. Landau, *Phys. Rev. B* 54 (1996) 12302.